Journal of Mechatronics, Electrical Power, and Vehicular Technology 16 (2025) 220-232

Journal of Mechatronics, Electrical Power, and Vehicular Technology

e-ISSN: 2088-6985
p-ISSN: 2087-3379

mev.brin.go.id

Design and implementation of a synchronous buck DC–DC converter with incremental conductance MPPT for green hydrogen production via PEM electrolysis

Novan Akhiriyanto *, Rizky Muhammad Afandi

Refinery Instrumentation Engineering Study Program, Energy and Mineral Polytechnic (PEM) Akamigas
Jalan Gajah Mada No. 38 Cepu, Blora, 58315, Indonesia

Abstract

The integration of green hydrogen production systems with photovoltaic (PV) energy sources presents challenges due to voltage mismatches between commercial solar charge controllers and the required input of proton exchange membrane (PEM) electrolyzers. This study presents an experimental implementation of a maximum power point tracking (MPPT) module using the incremental conductance (INC) algorithm embedded in a parallel buck converter configuration. The objective is to supply a stable low-voltage, high-current input to a PEM electrolyzer from a solar-powered system. The system employs three parallel-connected buck converters, each operating within a 3 V to 7 V range and capable of delivering up to 20 A and 60 W to 120 W per module. Combined, the converters manage a power range of 180 W to 360 W to match the electrolyzer's requirements under variable irradiance. The MPPT algorithm actively adjusts duty cycles to maintain the PV panel's output near its optimal power point, targeting 150 W to 210 W. Voltage, current, and power readings from both PV and converter sides are acquired in real time via PZEM-017 sensors. Testing was performed over a three-hour period during peak solar irradiance (10:40 AM–1:40 PM) to ensure observation within the maximum power window. The average output from the parallel buck converter was 4.36 V, 25.41 A, and 111.26 W, while the PV panel delivered 154.41 W. Real-world system efficiency ranged from 59.48 % to 70.04 %, with a peak potential of 72.05 %. These results confirm the viability of using a parallel buck converter controlled by INC MPPT to drive a PEM electrolyzer in green hydrogen applications. The findings also indicate opportunities to further enhance efficiency through system refinement and control optimization.

Keywords: green hydrogen; incremental conductance (INC); maximum power point tracking (MPPT); parallel buck converter; proton exchange membrane (PEM) electrolyzer.

I. Introduction

Green hydrogen is poised to play a pivotal role in the global effort to reduce carbon emissions and transition to sustainable energy sources. Furthermore, it plays a pivotal role in the storage of renewable energy and is important for chemical manufacturing [1]. Hydrogen, along with direct electrification and efficiency enhancements, will have a significant impact on reducing carbon emissions. To facilitate decarbonization in these sectors, we must produce them with minimal greenhouse gas emissions [2].

* Corresponding Author. akhiriyanto.n@gmail.com (N. Akhiriyanto)

https://doi.org/10.55981/j.mev.2025.1119

Received 27 September 2025; revised 18 November 2025; accepted 19 November 2025; available online 24 December 2025

How to Cite: N. Akhiriyanto and R. M. Afandi, "Design and implementation of a synchronous buck DC–DC converter with incremental conductance MPPT for green hydrogen production via PEM electrolysis," *Journal of Mechatronics, Electrical Power, and Vehicular Technology*, vol. 16, no. 2, pp. 220-232, Dec. 2025.

Therefore, producing hydrogen from water electrolysis with power from renewable energy sources clearly emerges as a preferred option.

The research investigates hydrogen gas production through water electrolysis as a potential alternative fuel for motorcycles [3]. Researchers view using solar energy to produce hydrogen as a potential strategy to harness solar energy and mitigate climate change resulting from fossil fuel combustion. Researchers have primarily explored photocatalytic technologies, photoelectron chemistry, photovoltaic-electrochemistry, solar thermochemistries, photothermal catalysts, and photobiological methods for producing solar-based hydrogen [4]. Using electroplating wastewater to manufacture hydrogen is considered an innovative strategy that aims to develop sustainable energy solutions while also addressing environmental problems [5].

Electrolysis methods differ depending on the electrolyte material and charge carrier: (1) alkaline electrolysis, widely available commercially; (2) proton exchange membrane (PEM) electrolysis, also commercially available; (3) anion exchange membrane (AEM) electrolysis, currently in commercial development; and (4) solid oxide (SO) electrolysis, still primarily in laboratory research stages [6][7]. Alkaline electrolysis and PEM electrolysis are currently the two leading commercially available technologies. Alkaline electrolysis is the most mature and widespread compared to PEM electrolysis because it has a longer life [8]. Nevertheless, PEM electrolysis has several advantages over alkaline electrolysis, such as compactness, fast system response, wide partial load range, and high flexibility in terms of operation [9]. This technology is an attractive option for integration into the power grid, including renewable power generation systems [10][11]. Thus, PEM electrolysis has been considered for use in this study.

When hydrogen is created by electrolysis with renewable energy sources, it is considered environmentally beneficial. The use of solar energy has significant promise for achieving this purpose. The intensity of solar radiation fluctuates naturally due to its intermittent nature, which significantly affects the efficiency of photovoltaic (PV) solar panels [12][13]. PV-powered PEM efficiency of electrolyzers plays a key role in minimizing the production cost of green hydrogen. Commercial crystalline silicon (c-Si) or monocrystalline solar cells have reached their maximum efficiency [14]. To minimize the cost of green hydrogen production, in addition to the maturity of PV technology, another equally significant factor is the regulatory framework for green hydrogen technology [15]. Renewable energy applications have enormous promise, but there are still important obstacles that need to be addressed. These include cutting prices, boosting efficiency, and developing better storage and transportation systems [16][17].

In a recent comparative study, the fuzzy logic controller (FLC)-based maximum power point tracking (MPPT) approach demonstrated a system efficiency of 98.73 %, slightly surpassing perturb and observe (P&O) at 96.63 %, while incremental conductance (INC) yielded 97.22 %. These results underscore the adaptability of FLC under variable conditions, although differences with INC remain within marginal bounds [18][19][20][21]. Temperature also has a significant impact on PV system performance; greater temperatures result in lower output and efficiency [22]. Thus, MPPT modules based on power electronics components are needed for the solar-powered green hydrogen synthesis process. According to the electrolytic specifications, the MPPT module will control the voltage of the solar PV output to keep it at the desired working voltage. This document provides the background information for developing MPPT modules that optimize the output of the green hydrogen system, which operates on the principle of electrolysis [23][24].

However, maximum efforts have been made to overcome these obstacles by looking for alternatives to overcome the problems. In situations like this, creative solutions can be applied to ensure that the process of prototyping this research continues to run according to the plan and flow set. At times, modifications may be required to the design to accommodate any changes or challenges that arise during the implementation process. PV panels are unable to attain their optimal performance during foggy scenarios in the absence of MPPT [25][26].

Power electronics technology, especially DC-DC converters, has experienced expansion in its application. Like power transformers in AC systems, DC-DC converter devices can change the desired DC voltage level. DC-DC converter which is also often referred to as DC chopper, is broadly made into 3 groups, namely: (1) boost converter which is able to increase the DC voltage level, (2) buck converter which is able to lower the DC voltage level, and (3) buck-boost converter which is able to raise or lower the DC voltage we want.

In this study, in order to be able to adjust the DC voltage required by the PEM electrolyzer which tends to be low with a large current flow compensation, if the desired power is the same as the main energy source, it requires a buck converter device that is able to drastically lower the DC voltage level of the PV panel so that it is in accordance with the voltage required by

the PEM electrolyzer and is able to withstand the large current flow absorbed by the PEM electrolyzer in order to produce optimal hydrogen gas production.

The concept of interleaving of the DC-DC converter has been used in order to reduce the voltage and current stress generated in the boosting process. From the point of view of a buck converter, the concept of interleaving is similar to connecting parallel buck converter devices so that they have sufficient capabilities to conduct large currents with low voltages.

A fairly basic difference from the study is that the boost converter device is designed as if it combines two boost converter circuits with a two-step boosting process. In this proposed study, it connects three buck converter circuits are connected in parallel in order to increase the ability to conduct a larger current by three times the specifications of the buck converter circuit, with a current capacity of 20 A [27].

In this research, the target output voltage supplied to the PEM electrolyzer was set at 5 V, with a target operating current of approximately 25 A to 30 A. Based on these parameters, the target output power to be maintained by the MPPT-controlled buck converter was in the range of 110 W to 150 W, aligned with the PV module's maximum power capability of around 150 W to 210 W. Furthermore, the system was designed to achieve a desired conversion efficiency of approximately 70 % during real-world operation.

II. Materials and Methods

Green hydrogen is produced from the electrolysis process of environmentally friendly renewable energy. Green hydrogen is formed from water separating into hydrogen and oxygen using an electric current. When electricity is produced from a source of sunlight, the hydrogen produced is the most environmentally friendly. Green hydrogen produces lower carbon emissions than grey hydrogen produced by natural gas vapour reforms, already coming in from the lion's market share. Some countries have tried to carbonize to meet net-zero emissions targets [28]. Decarbonization efforts require green hydrogen as it makes a significant contribution to industrial applications such as the manufacture of cement, ceramics, and glass. Green hydrogen is the central pillar because it is considered as important as battery storage (energy storage) in the future.

The experiment was conducted during peak solar irradiance, with data collected for approximately 3 h (10:40 AM–1:40 PM) around local solar noon to capture the maximum power window. This period corresponds to the typical "peak sun hours" (~4.8 h/d to 5.5 h/d) in Central Java, as regional irradiance commonly peaks between 11:00 and 13:00, with average daily GHI values of approximately 5.2 kWh/m²/d based on NASA POWER and Solargis data.

A. Electrolysis

Electrolysis is the decomposition of electrolytes in an electrolysis cell by an electric current. The process of electrolysis of data converts electrical energy into chemical energy. In addition, this process separates water molecules into hydrogen and oxygen gas by flowing an electric current to the electrode of the electrolyte solution, which consists of water and a catalyst. Produce oxygen (O_2), protons (H^+), and electrons (e^-). The O_2 produced is removed from the anodic surface, and the remaining H^+ flow through the proton-conducting membrane to the cathode side. e^- flow through an external circuit to the cathode side. The cathode sides of H^+ and e^- are combined back into a gas (H_2). The concept of electrolysis of PEM water is shown in Figure 1 [29].

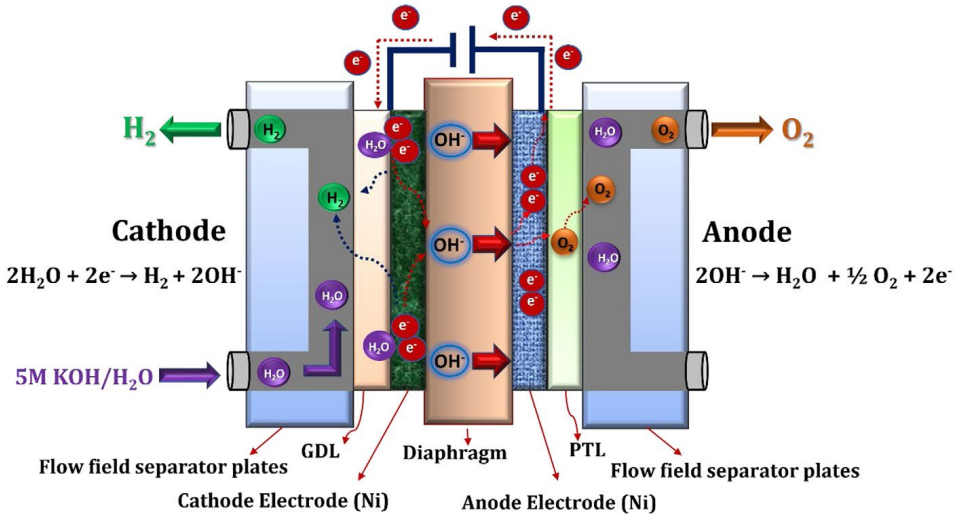

Figure 1. PEM water electrolysis.

B. Maximum power point tracking

The voltage-current (I-V) curve and power-voltage (P-V) curve, shows the relationship between voltage, current, power, and voltage generated by solar panels, as shown in Figure 2 [30]. MPPT is needed to maximize the power generated under certain irradiation conditions, which functions to find the optimal loading point. There is a nonlinear relationship between voltage and current in PV panels due to the influence of panel temperature and sunshine irradiation. Consequently, determining the ideal power-generating point requires the use of MPPT. The MPPT method commences by identifying the optimum voltage value that results in a specific current when multiplied by the voltage [31]. Subsequently, the product of voltage and current results in the generation of output power. The voltage is incrementally raised to optimize power until it reaches the maximum power point (MPP). The MPPT algorithm systematically raises the voltage in order to maximize the power output of the solar panel. This process persists as long as the irradiation parameters remain optimum. Enhancing the operational performance of solar panels at their greatest power points is crucial for optimizing system efficiency and maximizing electricity production.

In conclusion, the voltage-current curve in solar panels is affected by load characteristics, and MPPT is required to maximize output power. Irradiation and panel temperature also affect voltage and current, making the relationship nonlinear [32][33]. Through the gradual increase in voltage, MPPT can reach the MPP and ensure the working efficiency of solar panels [34][35][36].

C. Incremental conductance

The INC algorithm is the most optimal power point search algorithm by comparing the derivatives of power, voltage, and current values [37][38][39]. This algorithm uses voltage and current as input and then as a locator of the latest power value and the difference with the previous power value, as shown in Figure 3 [40].

- $dP/dU > 0$, the operating point is to the left of the maximum value, so it is necessary to increase the voltage
- $dP/dU < 0$, the operating point to the right of the MPP, a voltage drop is necessary
- $dP/dU = 0$, operating point at peak power point

Power is the product of the multiplication of voltage and current, expressed in equation (1).

$$\frac{dP}{dU} = \frac{d(U.I)}{dU} = I + \frac{U\Delta I}{\Delta U} \quad (1)$$

The INC technique is effective and fast for MPPT, as shown in Figure 4. The concepts at play are as follows:

- Point A, left of MPP: If the difference between the change in voltage (ΔU) and the change in current (ΔI) more than the negative ratio of current (I) to voltage (U), then the operating point is located to the left of the MPP. In this case, reaching the MPP will require raising the voltage or the duty cycle ($D_n + \Delta d$)
- Point B, right of MPP: The operating point is to the right of the MPP if the difference between ΔU and ΔI is smaller than the negative ratio of I to U. In this case, reaching the MPP requires lowering the voltage or the duty cycle ($D_n - \Delta d$)
- At MPP (point MPP): The system is at the MPP if the difference between ΔU and ΔI equals the negative ratio of I to U. In this case, the duty cycle is constant because the optimal power generation point has already been reached

The INC algorithm's high accuracy and ease of use in energy optimization make it a fantastic choice for MPPT systems. The INC algorithm ensures optimal performance of solar panels under various climatic conditions by continuously monitoring and adjusting the operating point in compliance with the prescribed specifications.

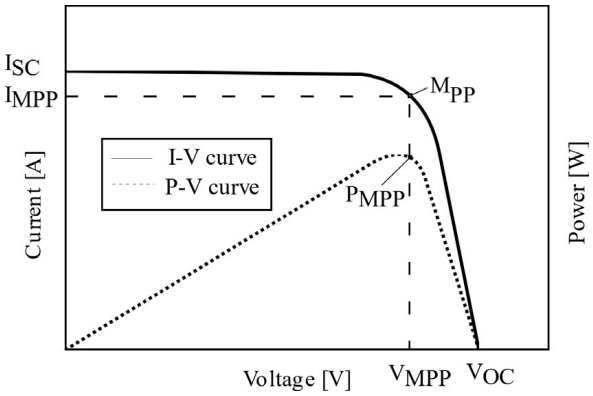

Figure 2. I-V and P-V curve of solar PV.

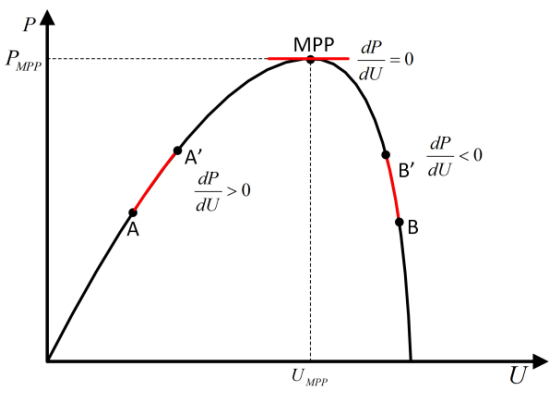

Figure 3. INC algorithm graph.

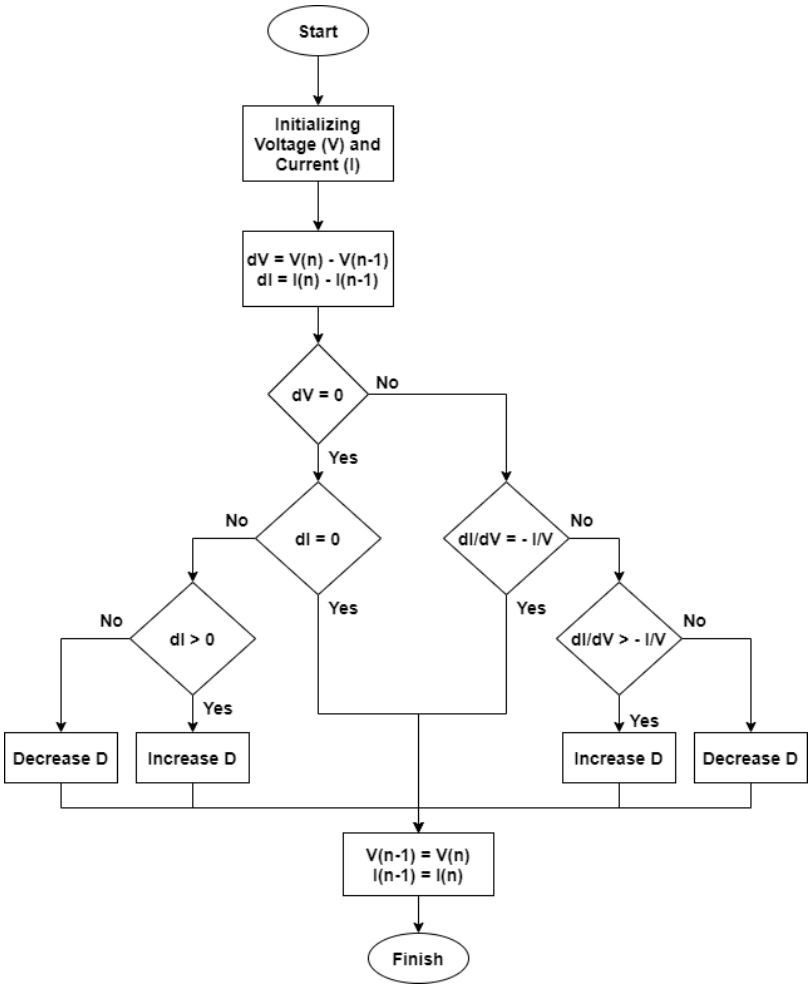

Figure 4. INC flowchart.

D. Parallel buck converter modules

This system employs three parallel buck converters functioning as voltage and current conditioners from the solar panel to the electrolyzer. Conventionally, voltage regulation in the synchronous buck converter is performed by manually adjusting a variable resistor (as shown in Figure 5) to achieve the desired output voltage. For automatic regulation, the module was modified by adding a servo-driven potentiometer. This mechanical approach was chosen because the internal gate-drive circuitry of the commercial buck module cannot be accessed directly.

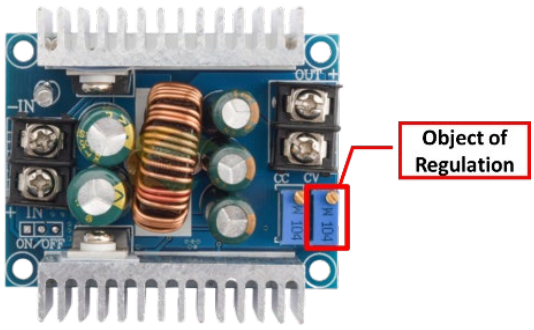

Figure 5. CV variable resistor location.

As shown in Figure 5, the buck converter used in this study, commonly available in the market, is the LM25116, a wide input range synchronous buck controller rated for 6 V to 100 V input. It features an adjustable output voltage typically ranging from 0.8 V to 90 V, depending on external feedback resistor configuration, programmable switching frequency up to 750 kHz, and supports output currents exceeding 20 A, depending on external components. The device integrates peak current-mode control with adaptive slope compensation, internal 7.7 V gate drivers, soft-start control, and adjustable current limit, making it suitable for high-efficiency PV to electrolyzer DC conversion under real-world dynamic conditions.

The LM25116 controller does not include a dedicated onboard interface for constant voltage (CV) or constant current (CC) tuning via a potentiometer. However, adjustable output voltage CV can be implemented by replacing one of the feedback resistors (RFB1 or RFB2) with a trimpot, as these define the output voltage through the feedback network to the FB pin (as shown in Figure 6). Similarly, the current limit CC can be tuned by modifying the sense resistor (RS), where inserting a variable resistor in series or parallel

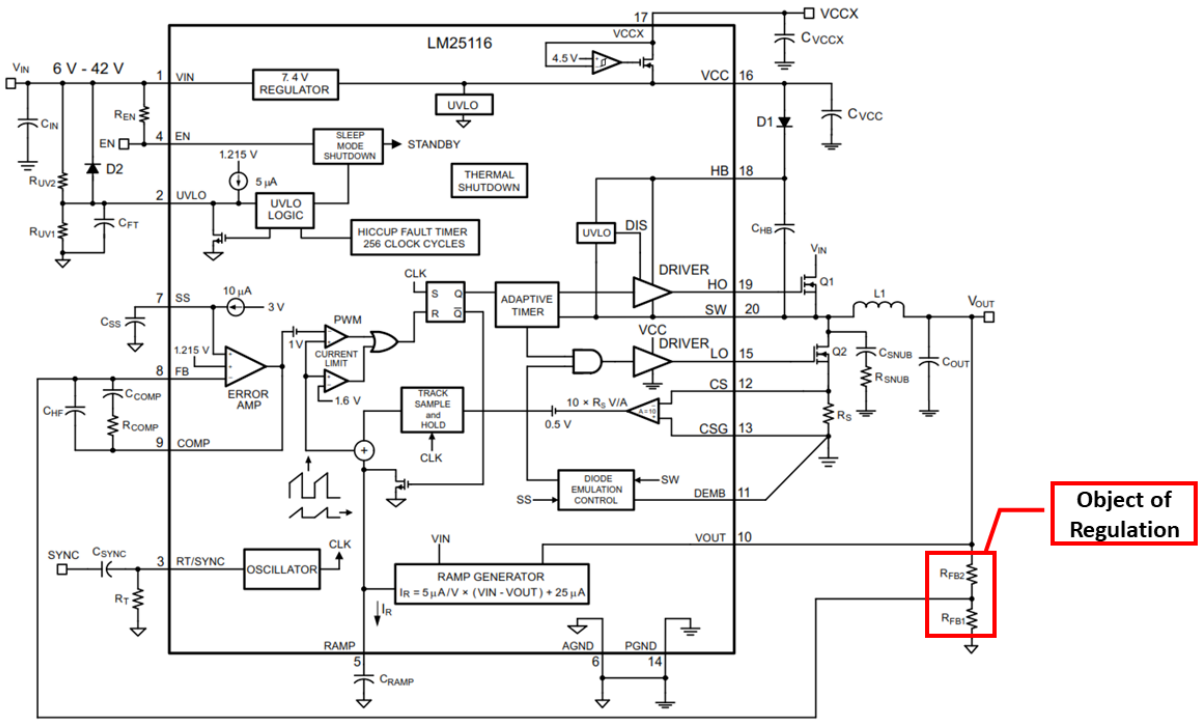

Figure 6. LM25116 schematic diagram.

with RS enables manual adjustment of the peak current threshold sensed at the CS and CSG pins.

The mechanism works by coupling the potentiometer lever with the servo, such that adjusting the servo's angle causes the potentiometer to change accordingly, as illustrated in Figure 7.

This modification enables the buck converter to perform automatic voltage regulation by adjusting the potentiometer position according to the algorithm's output. The mechanical method was implemented because the internal switching and gate-drive circuitry of the commercial buck converter module could not be accessed directly. In principle, the mechanical system is not required, and it would be far more effective for the control signal generated by the INC algorithm to be integrated directly into the metal-oxide-semiconductor field-effect transistor (MOSFET) gate drive of the converter. However, due to hardware constraints, the servo-driven adjustment provided a practical workaround for prototyping, allowing the converter to follow the voltage and current requirements of the PEM electrolyzer. Future development will eliminate the mechanical mechanism entirely and implement direct electronic control to improve efficiency and response time.

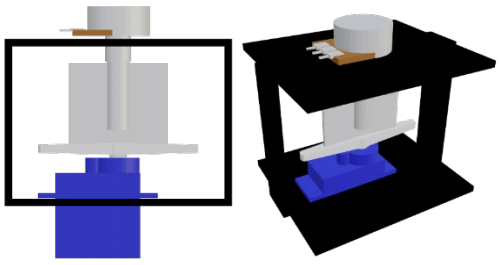

Figure 7. Potentiometer coupled by servo motor.

A PZEM module is used to measure the input and output parameters of the buck converter, providing essential data for MPPT regulation. The Nextion display functions as an interface for monitoring and controlling MPPT performance, presenting key data such as the input-output voltage and current of the buck converter while also allowing users to configure the MPPT operating mode. All components are housed in an electrical panel box with a layout as shown in Figure 8.

E. Architecture of the proposed approach

In this study, the MPP voltage of the PV panels is 38.2 V_{mpp}, but the PEM electrolyzer, the main load in the system, requires only 3 V to 7 V. The PZEM-017 sensor module, known for its reliable precision, ensures accurate voltage and current readings. The PZEM-017 sends voltage and current data from the PV panels to the ESP32 microcontroller, which then calculates and provides the voltage, current, and power values. First, the measured power value is compared with the buck converter to determine the resistance setting. Reaching the MPP of the PV module is the aim of this resistance setting. The voltage, current, and power values at the parallelized buck converter output and the solar module output are displayed on the Nextion LCD, as seen in Figure 9.

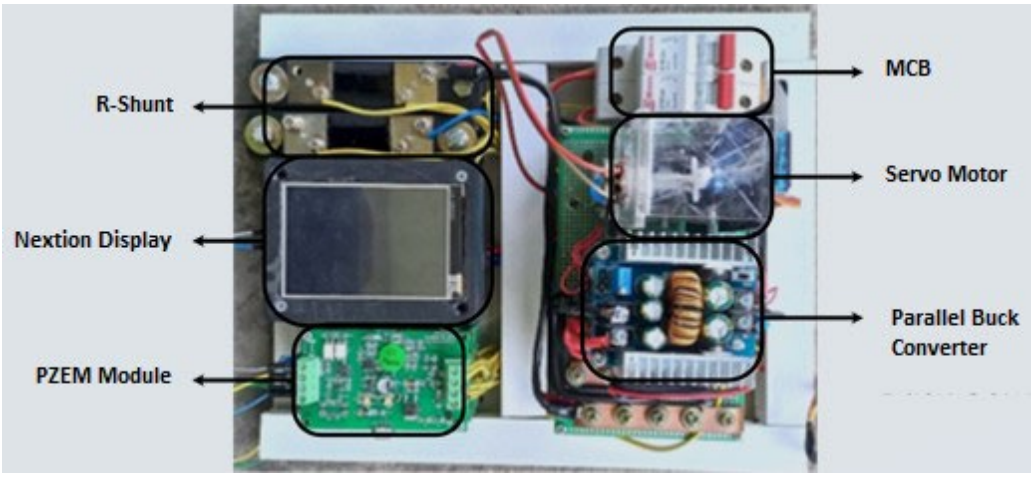

Figure 8. Overall electrical components.

Based on Figure 9, the hardware requirements to build this system consist of input section, the PV panel serves as the primary power generator in the system, with a maximum power output of 250 Wp, a maximum power point voltage (V_{mpp}) of 38.3 V with an open-circuit voltage (V_{oc}) of 45.8 V, and a current (I_{mpp}) of 6.55 A with a short-circuit current (I_{sc}) of 6.98 A then processing section, this section comprises two PZEM-017 sensor modules used to measure the voltage and current from the input and output of the main buck converter, which is the main focus of this study, a 5 V buck converter module is also included, which transforms the voltage from the PV panel output to power the ESP32 microcontoller. In order to operate the main buck converter and the 12 V buck converter module, which transforms the voltage from the PV panel output to power the DC pump, this microcontroller transmits a duty cycle signal. Last, the output section, section consists of the main electrical load, the PEM electrolyzer, which requires a 5 V DC supply as the setpoint output for the main buck converter. It also features a Nextion LCD monitor and a DC pump to supply water to the PEM electrolyzer. The DC pump in the system functions to continuously circulate distilled water into the PEM electrolyzer during hydrogen production.

The main function of the main buck converter is to compensate for voltage drops in the PV panel and supply the PEM electrolyzer with an output voltage of 5 V. Unlike the others, this primary buck converter module is built to tolerate a maximum current of 60 A.

The system's functionality to be created can run properly, and a study is needed that involves the configuration of specific sensors as a source of measurable data. In this context, the research requires using microcontrollers to retrieve the required parameter values. Python was selected as the programming language to carry out this configuration because it works with ESP32 microcontrollers, as Figure 10 illustrates. The data flow from these sensors

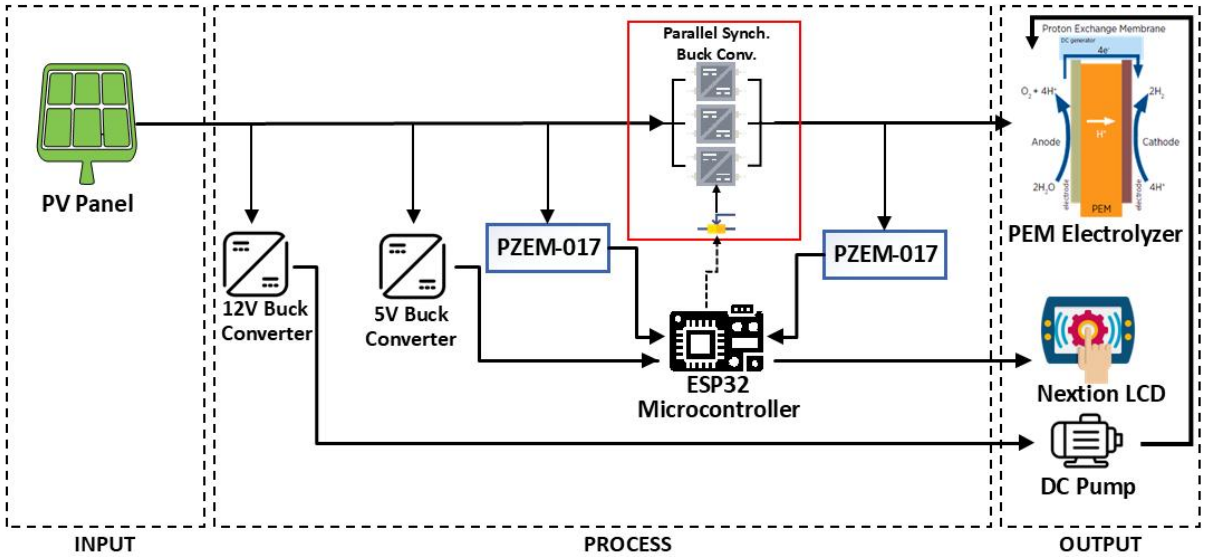

Figure 9. Architecture of the proposed approach.

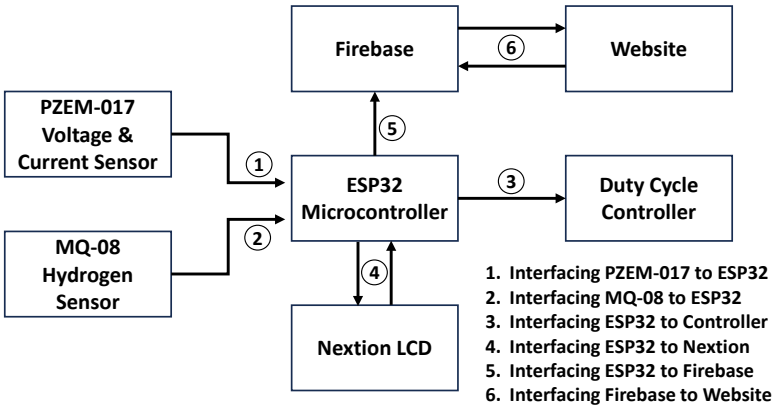

Figure 10. Interface architecture.

was regulated and controlled by the study using ESP32 and Python. It makes it possible for the system to gather and use pertinent data for the intended use.

The study incorporates both mechanical and electrical works in its hardware design. The hardware overall design in the real world for the PV panel frame structure, as depicted in Figure 11. This entails identifying the most efficient dimensions, configuration, and placement of the PV panels in order to optimize the capture of solar energy. After the design is completed, the frame structure is built based on the design parameters, utilizing metal materials to provide support and safeguard the PV panels and other components.

The mechanical work also includes the arrangement of numerous auxiliary components, such as water tanks, hydrogen tanks, an electrical panel box, and cable ducts. Ensuring the correct positioning of these elements is essential for upholding the system's overall efficiency and security. The water and hydrogen tanks are strategically positioned to ensure easy access,

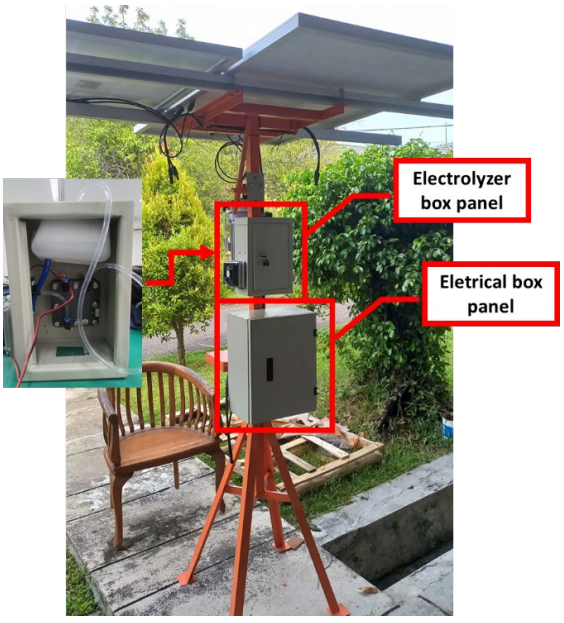

Figure 11. Hardware overall design.

efficient piping connections, and safeguard against adverse weather conditions and external factors. The purpose of the electrical panel box is to protect electrical and electronic components from potential harm. Finally, cable ducts are installed to protect the cables that link various components of the system.

III. Results and Discussions

Data was submitted to the database every ten seconds throughout the roughly 9800 s that the study's proposed system ran from 10:40 am to 1:40 pm. Real-world conditions were observed, and the voltage and current magnitudes were determined as indicated in Figure 12.

The main buck converter converts the output voltage of the PV panel (in Figure 12 called PV voltage) has an average value of 35.11 V into the input voltage required by the PEM electrolyzer (called PEM elect. voltage) has an average value of 4.36 V. While the output current of the PV panel (called PV current) has an average value of 4.30 A compensated by changing the voltage by the main buck converter so that the input current to the PEM electrolyzer (called PEM Elect Current) becomes greater, has an average value of 25.41 A.

A. Real-world characteristics of voltages and currents

As shown from the observation data in Figure 12, the main buck converter is relatively able to maintain the input voltage of the PEM electrolyzer in accordance with the setpoint, which is 5 V. Although, the average input voltage PEM electrolyzer has a value of 4.36 V with a maximum voltage value of 5.3 V. Unlike the input voltage of the PEM electrolyzer which has a tendency to be kept constant according to the previous description, the input current to the PEM electrolyzer varies sometimes drastically even though it does not follow the variation in the voltage and output current

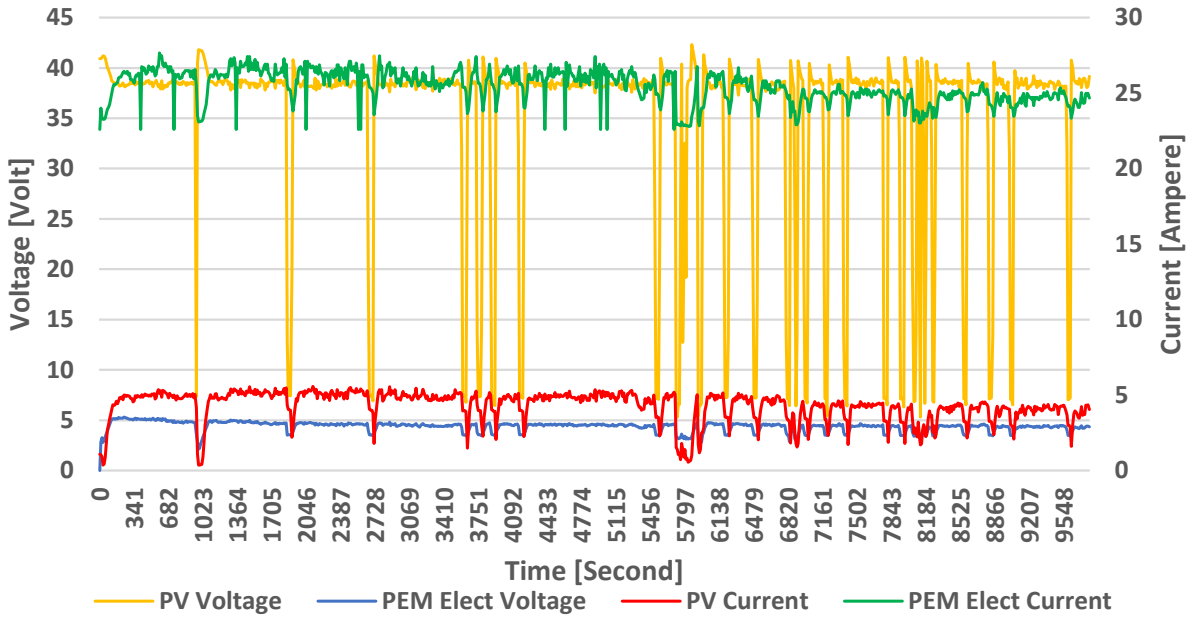

Figure 12. Voltage and current characteristics.

of the PV panel, but the input current to the PEM electrolzyer tries to follow the output voltage value of the PV panel, although the maximum input current of the PEM electrolyzer is only able to reach 27.66 A.

The output voltage and current characteristics of PV panels have a maximum value of 42.32 V and 5.57 A. However, when the PV panel decreases dramatically in the 5720th second is worth 5.32 V far below its average value of 35.11 V, then the PV panel output current also decreases to 1.39 a below the average value of 4.30 V and does not seem to apply otherwise, if the minimum output current of the PV panel decreases dramatically to 0.36 A which occurs in the 990th second, then the PV panel output voltage is still high at 41.78 V.

Although there are still many ripples caused by the intermittency of the voltage and current of the PV panel as the main energy source, overall, the main buck converter has worked effectively by keeping the input voltage of the PEM electrolyzer around the setpoint of 5 V.

B. Real-world characteristics of power

From the observation data in Figure 10, then calculated the value of power by multiplying the value of voltage and current, so as to obtain the results of characteristics such as Figure 13. The power characteristics that the PEM electrolyzer absorbs (in Figure 13 called PEM elect. power) as the main load in

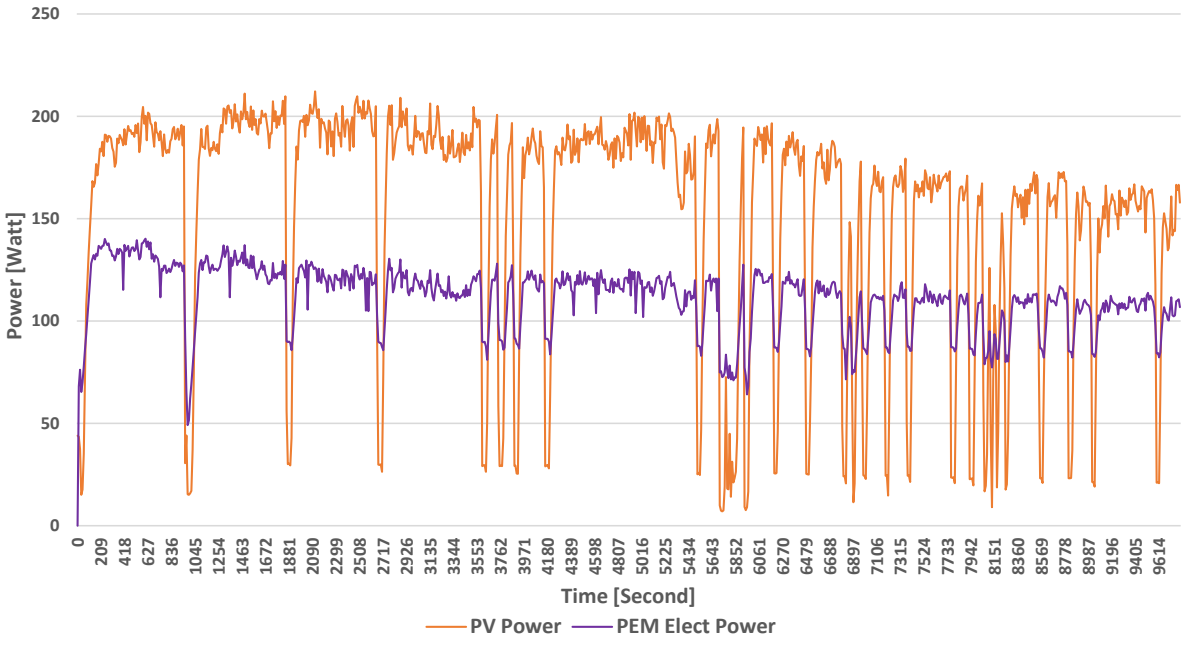

Figure 13. Power characteristics.

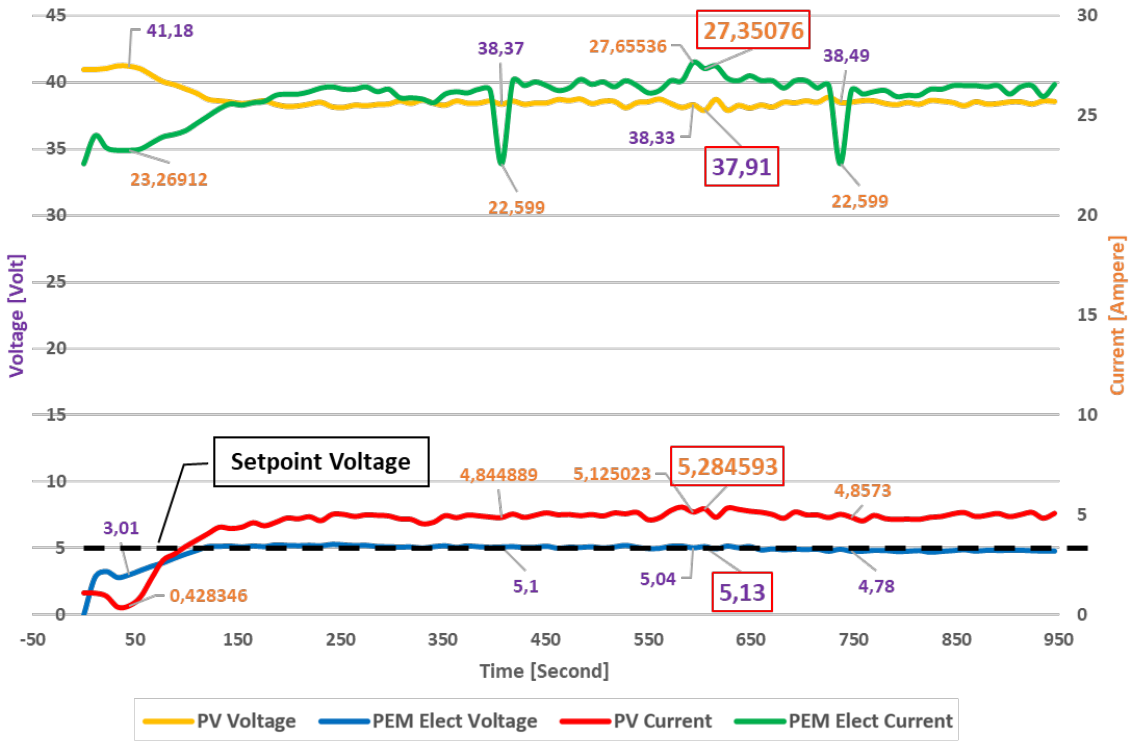

Figure 14. Efficiency when the electrolyzer absorbs maximum power.

the proposed system always follow the PV panel power (called PV power). If PV power has decreased the value of power drastically, then PEM elect. power always follows the PV power value, even if the PEM elect. power value is below the PV power value.

From the observation data, it was obtained that the average power generated by the PV panel was 154.41 W with a maximum power of 212.25 W, while the average value of the power absorbed by the PEM electrolyzer was 111.26 W with a maximum power of 140.31 W.

C. Efficiencies of the proposed approach

Based on the results of observation data shown by Figure 10, there are two conditions that occur so that they have a misaligned relationship that is the basis of the main focus in the discussion of the efficiency of this proposed approach, namely: (1) when the power consumed by the PEM electrolyzer reaches its maximum value; and (2) when the power generated by the PV panel reaches its maximum value. And in general, also add the calculation of efficiency seen from the amount of average power.

When the power consumed by the PEM electrolyzer reaches the maximum value occurs in the 605th second with a voltage value of 5.13 V, and the current flowing to the PEM electrolysis reaches about 27.35 A. It turns out that the voltage generated by the solar panel is 37.19 V and flows a current of 5.28 A, can be seen in Figure 14. Each of the powers generated by the PV panel is considered as input power, while the power absorbed by the PEM electrolyzer is considered as output power, so because of the DC system, the power can be found by multiplying the voltage and current values. Then to calculate the efficiency, it can be divided the output power by the input power. Then, the efficiency when the PEM electrolyzer absorbs the maximum power reaches about 70.04 %.

Meanwhile, when the power generated by the PV panel reaches the maximum value occurs in the 2112th second with the voltage generated reaching 38.13 V and a current of about 5.57 A, it turns out that the power consumed by the PEM electrolysis has a voltage of 4.71 V and the current flowing to the PEM electrolyzer reaches about 26.80 A, can be seen in Figure 15.

Based on the target setpoint of 5.00 V and the observed steady state output of 4.71 V. This deviation is attributed primarily to real-world fluctuations in solar irradiance and temperature during operation. Although the 5.8 % steady-state error indicates a slight voltage drop from the reference setpoint, the achieved output (4.71 V) remains sufficient to drive the electrochemical reaction in the PEM electrolyzer, which typically operates effectively above 4.5 V under load. Therefore, regulation performance is considered acceptable within the context of outdoor PV-powered electrolysis. With the same assumption, the efficiency when the PV panel produces its maximum power reaches about 59.48 %.

Finally, in general, from the point of view of the average value of the input power generated by the PV

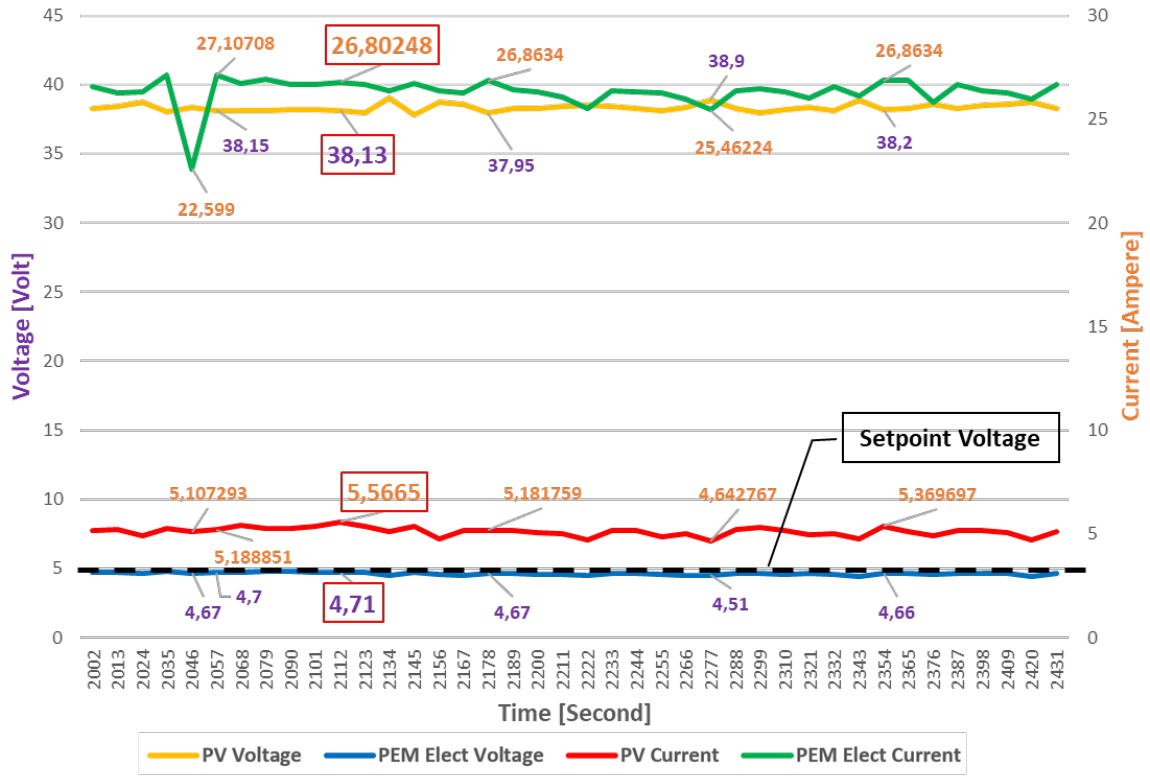

Figure 15. Efficiency when the PV panel generates maximum power.

panel is 154.41 W and the output power absorbed by the PEM electrolyzer is 111.26 W, the efficiency reaches about 72.05 %, with observation data for 9801 s or about 3 h.

IV. Conclusion

This study presents the implementation of a PV-powered hydrogen production system using a synchronous parallel buck converter controlled by the INC MPPT algorithm. The system maintained an average electrolyzer input voltage of 4.36 V and current of 25.41 A, with an output power of 111.26 W relative to the PV panel's average power of 154.41 W. The corresponding real-world efficiency ranged from 59.48 % to 70.04 %, with a potential average of 72.05 %. These results indicate that the MPPT control not only stabilizes voltage and current but also sustains power delivery to the electrolyzer within the 110 W to 150 W range under variable irradiance. The conclusion is consistent with the research objectives, which include regulating voltage, current, and delivered power under actual environmental conditions. Further exploration of metaheuristic MPPT algorithms, such as the firefly algorithm, genetic algorithm (GA), differential evolution (DE), or particle swarm optimization (PSO), is recommended to enhance performance under partial shading and dynamic weather variations.

Acknowledgements

The authors thank Energy and Mineral Polytechnic (PEM) Akamigas under the Ministry of Energy and Minerals, which, in general, has made it easier to allocate budget for our research. Of course, because we conduct research vocationally, it is expected that the results of this research and study can be useful to the community in the future, related to applied technology in applying environmentally friendly hydrogen as one of the new energy sources.

Declarations

Author contribution

N. Akhiriyanto: Writing – Review and Editing, Conceptualization, Investigation, Visualization, Supervision, Funding acquisition. **R.M. Afandi**: Writing – Original Draft, Formal Analysis, Investigation, Visualization, Validation, Data Curation, Software.

Funding statement

This paper is funded by the Energy and Mineral Polytechnic Akamigas (PEM Akamigas) under the Ministry of Energy and Minerals of Republic of Indonesia grant no. 028/SP3/Penelitian/DIPA2023/PEM Akamigas.

Competing interest

The authors declare that they have no known competing financial interests or personal relationships that could have appeared to influence the work reported in this paper.

The use of AI or AI-assisted technologies

During the preparation of this work the authors used ChatGPT 5.2 to translate and paraphrase the manuscript's English grammar, while the original concepts were drafted by the authors. After using this tool/service, the authors reviewed and edited the content as needed and take full responsibility for the publication.

Additional information

Reprints and permission: information is available at https://mev.brin.go.id/.

Publisher's Note: National Research and Innovation Agency (BRIN) remains neutral with regard to jurisdictional claims in published maps and institutional affiliations.

References

[1] A. H. Azadnia, C. McDaid, A. M. Andwari, and S. E. Hosseini, "Green hydrogen supply chain risk analysis: A european hard-to-abate sectors perspective," *Renew. Sustain. Energy Rev.*, vol. 182, no. May, p. 113371, 2023.

[2] Y. Zhang, Y. Xiao, S. Abuelgasim, and C. Liu, "A brief review of hydrogen production technologies," *Clean Energy Sci. Technol.*, vol. 2, no. 1, p. 117, 2024.

[3] Zikri, A. Derisman, Muslim, W. Purwanto, and A. I. Imran, "Study on the production of hydrogen gas from water electrolysis on motorcycle engine," *J. Mechatronics, Electr. Power, Veh. Technol.*, vol. 13, no. 1, pp. 88–94, 2022.

[4] H. Song, S. Luo, H. Huang, B. Deng, and J. Ye, "Solar-driven hydrogen production: Recent advances, challenges, and future perspectives," Mar. 11, 2022, *American Chemical Society*.

[5] R. Rusdianasari, A. Taqwa, A. Syarif, and Y. Bow, "Hydrogen recovery from electroplating wastewater electrocoagulation treatment," vol. 13, no. 2, 2023.

[6] A. M. I. Noor Azam *et al.*, "Parametric study and electrocatalyst of polymer electrolyte membrane (PEM) electrolysis performance," *Polymers (Basel).*, vol. 15, no. 3, 2023.

[7] X. Wang, P. Mardle, M. Adamski, B. Chen, and S. Holdcroft, "Proton exchange membrane water electrolysis incorporating sulfo-phenylated polyphenylene catalyst coated membranes," *J. Electrochem. Soc.*, vol. 170, no. 2, p. 024502, 2023.

[8] L. Li *et al.*, "High-rate alkaline water electrolysis at industrially relevant conditions enabled by superaerophobic electrode assembly," *Adv. Sci.*, vol. 10, no. 4, pp. 1–7, 2023.

[9] J. Brauns and T. Turek, "model-based analysis and optimization of pressurized alkaline water electrolysis powered by renewable energy," *J. Electrochem. Soc.*, vol. 170, no. 6, p. 064510, 2023.

[10] B. Brigljević *et al.*, "When bigger is not greener: Ensuring the sustainability of power-to-gas hydrogen on a national scale," *Environ. Sci. Technol.*, vol. 56, no. 18, pp. 12828–12837, 2022.

[11] T. Koo, R. Ko, D. Ha, and J. Han, "Development of model-based PEM water electrolysis HILS (hardware-in-the-loop simulation) system for state evaluation and fault detection," *Energies*, vol. 16, no. 8, 2023.

[12] M. A. Khan, I. Al-Shankiti, A. Ziani, and H. Idriss, "Demonstration of green hydrogen production using solar energy at 28% efficiency and evaluation of its economic viability," *Sustain. Energy Fuels*, vol. 5, no. 4, pp. 1085–1094, 2021.

[13] Q. Hassan, I. S. Abdulrahman, H. M. Salman, O. T. Olapade, and M. Jaszczur, "Techno-economic assessment of green hydrogen production by an off-grid photovoltaic energy system," *Energies*, vol. 16, no. 2, 2023.

[14] J. Rey, F. Segura, and J. M. Andujar, "Green hydrogen: Resources consumption, technological maturity, and regulatory framework," *Energies*, vol. 16, no. 17, 2023.

[15] Q. Hassan, V. S. Tabar, A. Z. Sameen, H. M. Salman, and M. Jaszczur, "A review of green hydrogen production based on solar energy; techniques and methods," *Energy Harvest. Syst.*, vol. 11, no. 1, pp. 1–28, 2024.

[16] D. Freire Ordóñez *et al.*, "Quantifying global costs of reliable green hydrogen," *Energy Adv.*, vol. 2, no. 12, pp. 2042–2054, 2023.

[17] D. Hidouri, R. Marouani, and A. Cherif, "Modeling and simulation of a renewable energy PV/PEM with green hydrogen storage," *Eng. Technol. Appl. Sci. Res.*, vol. 14, no. 1, pp. 12543–12548, 2024.

[18] N. Pamuk, "Performance analysis of different optimization algorithms for MPPT control techniques under complex partial shading conditions in PV systems," 2023.

[19] K. Sabri, O. El Maguiri, and A. Farchi, "Comparative study of different MPPT algorithms for photovoltaic systems under partial shading conditions," no. October 2023, 2021.

[20] A. Badea, D. Manaila-maximean, L. Fara, and D. Craciunescu, "Maximizing solar photovoltaic energy efficiency: MPPT techniques investigation based on shading effects," *Sol. Energy*, vol. 285, no. November 2024, p. 113082, 2025.

[21] O. Timur and B. K. Uzundag, "Design and analysis of a hybrid MPPT method for PV systems under partial shading conditions," *Appl. Sci.*, vol. 15, 2025.

[22] M. Irwanto, A. W. W. Nugraha, N. Hussin, and I. Nisja, "Effect of temperature and solar irradiance on the performance of 50 HZ photovoltaic wireless power transfer system," *J. Teknol.*, vol. 2, pp. 53–67, 2023.

[23] P. Marocco, M. Gandiglio, and M. Santarelli, "Optimal design of PV-based grid-connected hydrogen production systems," *J. Clean. Prod.*, vol. 434, no. December 2023, p. 140007, 2024.

[24] M. Awad, M. M. Mahmoud, Z. M. S. Elbarbary, L. M. Ali, S. N. Fahmy, and A. I. Omar, "Design and analysis of photovoltaic/wind operations at MPPT for hydrogen production using a PEM electrolyzer: Towards innovations in green technology," *PLoS One*, vol. 18, no. 7 July, pp. 1–24, 2023.

[25] W. Jinpeng, Y. Qinxue, Z. Bo, Jeremy-Gillbanks, and Z. Xin, "Study on MPPT algorithm based on an efficient hybrid conjugate gradient method in a photovoltaic system," *IEEE Access*, vol. 11, no. December 2022, pp. 4219–4227, 2023.

[26] M. A. Rabbani, M. B. Qureshi, S. A. Al Qahtani, M. M. Khan, and P. Pathak, "Enhancing MPPT performance in partially shaded PV systems under sensor malfunctioning with fuzzy control," *Energies*, vol. 16, no. 12, 2023.

[27] F. Osselin, C. Soulaine, C. Fauguerolles, E. C. Gaucher, B. Scaillet, and M. Pichavant, "Orange hydrogen is the new green," *Nat. Geosci.*, vol. 15, no. 10, pp. 765–769, 2022.

[28] S. Shiva Kumar and H. Lim, "An overview of water electrolysis technologies for green hydrogen production," *Energy Reports*, vol. 8, pp. 13793–13813, 2022.

[29] J. I. Morales-Aragonés, M. Dávila-Sacoto, L. G. González, V. Alonso-Gómez, S. Gallardo-Saavedra, and L. Hernández-Callejo, "A review of I–V tracers for photovoltaic modules: Topologies and challenges," *Electron.*, vol. 10, no. 11, 2021.

[30] M. M. Farag *et al.*, "An optimized fractional nonlinear synergic controller for maximum power point tracking of photovoltaic array under abrupt irradiance change," *IEEE J. Photovoltaics*, vol. 13, no. 2, pp. 305–314, 2023.

[31] M. F. Tsai, C. S. Tseng, K. T. Hung, and S. H. Lin, "A novel DSP-based MPPT control design for photovoltaic systems using neural network compensator," *Energies*, vol. 14, no. 11, 2021.

[32] A. Chellakhi and S. El Beid, "High-efficiency MPPT strategy for PV systems: Ripple-free precision with comprehensive simulation and experimental validation," *Results Eng.*, vol. 24, no. October, p. 103230, 2024.

[33] S. Manna, D. Kumar, A. Kumar, and H. Kotb, "Design and implementation of a new adaptive MPPT controller for solar PV systems," *Energy Reports*, vol. 9, pp. 1818–1829, 2023.

[34] M. Majstorovic, D. Mrsevic, B. Duric, M. Milesevic, Z. Stevic, and Z. V. Despotovic, "Implementation of MPPT Methods with SEPIC Converter," *2020 19th Int. Symp. INFOTEH-JAHORINA, INFOTEH 2020 - Proc.*, no. July, 2020.

[35] A. Chellakhi, S. El Beid, and Y. Abouelmahjoub, "Implementation of a novel MPPT tactic for PV system applications on Matlab / Simulink and proteus-based arduino board environments," vol. 2021, 2021.

[36] G. Hasan, A. Uddin, A. H. M. I. Ferdous, and G. Sadeque, "Enhanced maximum power point tracking using hybrid GA and PSO algorithms for solar PV systems," *Results Eng.*, vol. 28, no. October, p. 107708, 2025.

[37] M. Abu *et al.*, "Implementation of incremental conductance MPPT algorithm with integral regulator by using boost converter in grid-connected PV array," no. May, 2021.

[38] H. Yatimi and S. Chahid, "Design of an incremental conductance maximum power point tracking controller based on automation PLC for PV applications," no. June, pp. 12–13, 2021.

[39] J. Alonso *et al.*, "Development and implementation of the MPPT based on incremental conductance for voltage and frequency control in single-stage DC-AC converters," *Energies*, vol. 18, p. 184, 2025.

[40] S. A. Gorji, "Reconfigurable quadratic converters for electrolyzers utilized in DC microgrids," *IEEE Access*, vol. 10, no. September, pp. 109677–109687, 2022.